Colloid and Polymer Science (2021) 299:855–863
https://doi.org/10.1007/s00396-021-04811-y

ORIGINAL CONTRIBUTION

Microplasma synthesis of silver nanoparticles in PVP solutions using sacrificial silver anodes

O. I. Kuntyi[1] · A. R. Kytsya[2] · A. B. Bondarenko[1] · A. S. Mazur[1] · I. P. Mertsalo[1] · L. I. Bazylyak[2]

Received: 17 May 2020 / Revised: 22 December 2020 / Accepted: 6 January 2021 / Published online: 17 January 2021

Abstract

The method of contact glow discharge with the using of "sacrificial" silver anodes have been proposed for synthesis of silver nanoparticles (AgNPs) stabilized by polyvinylpyrrolidone (PVP). Using transmission electron microscopy, it was found that the mean size of AgNPs decrease from 10 to 5 nm with increasing of PVP concentration from 2.5 to 10 g/L. At the same time, the polydispersity index of AgNPs non-monotonically depends on concentration of stabilizer and the narrowest size distribution (less than 15%) was observed at PVP concentration equal to 5 g/L. The electrochemical investigations of Ag anodic dissolution associated with the recorded UV-Vis spectra of the obtained AgNPs solutions suggest that (i) the rate of silver dissolution depend on the nature of regulating agent—NaOH or CH_3COONa; (ii) silver anodes are not passivated in the presence of PVP; (iii) unlike to the process of chemical reduction of silver ions by PVP using of the contact glow discharge technique provides a pseudo-stationary process mode, i.e., the stability of rates of nucleation and growth of AgNPs via stability both of Ag^+ and solvated electrons concentrations that leads to formation of nearly monodisperse nanoparticles.

Keywords Silver nanoparticles · PVP · Glow discharge · "Sacrificial" silver anode · Kinetics

Introduction

Currently, the most studied methods to obtain colloidal solutions of metal nanoparticles (MNPs) are those based on chemical reduction of metallic salts using various inorganic compounds [1–4]. Moreover, in the last decade, much attention has been paid to the "green" synthesis of MNPs involving more environmentally friendly reagents [5, 6]. In general, the process of nanoparticle formation carried out through sequence successive steps: (1) reduction of M^{n+} ions into the atoms of M^0; (2) the compounding of atoms into nanoclusters (MNCs), i.e., nucleation; (3) growth of MNCs and formation of MNPs. All of these stages are multifactorial and difficult to control, especially the concentrations of the reducing agent and the metal ions which are the main parameters of mass transfer during the nucleation and growth of nanoparticles [7]. Therefore, using chemical reduction techniques, it is difficult to control the size and shape of MNPs that define physical, catalytic, antibacterial, and other properties [8, 9]. These problems—changing of concentrations of precursors—partially can be solved by electrochemical methods of MNPs synthesis [10–15] in particular those ones that used concentrated energy flows, for example microplasma electrolysis [16–23]. In addition, such methods minimize the number of precursors by using of sacrificial anodes as the source of metal ions. Therefore, the electrochemical synthesis of MNPs may be referred to "green" techniques. Thus, thorough studies of electrode processes during such synthesis are one of the important tasks of the electrochemistry of metal nanoparticles and especially silver nanoparticles due to their wide using.

Electrochemical reduction of metallic ions (that are formed via reaction 1) under conditions of electrochemical discharge in aqueous solutions (plasma in aqueous solutions) occurs in the bulk of the solution. Such nature of the process is due to the fact that the generated in microplasma electrons easily hydrates in aqueous medium (reaction 2) and then can reduce ions of metal M^{n+}

✉ A. R. Kytsya
kytsya@nas.gov.ua; andriy_kytsya@yahoo.com

[1] Department of Chemistry and Technology of Inorganic Substances, Lviv Polytechnic National University, Bandery Str. 12, Lviv 79013, Ukraine

[2] Department of Physical Chemistry of Fossil Fuels of the Institute of Physical-Organic Chemistry and Coal Chemistry named after L. M. Lytvynenko of the National Academy of Sciences of Ukraine, Naukova Str. 3a, Lviv 79060, Ukraine

(reaction 3) [17]. Then (by analogy to chemical reduction), metal atoms are combined into nanoclusters (nucleation of nanoparticles) subsequent by growth and agglomeration (reaction 4) that leads to formation of nanoparticles.

$$M^{n+} + ne^- \rightarrow M^0 \quad (1)$$

$$e^- + nH_2O \rightarrow e^-_{aq} \quad (2)$$

$$M^{n+} + ne^-_{aq} \rightarrow M^0 \quad (3)$$

$$M^0 \rightarrow M_2 \rightarrow \ldots \rightarrow M_x \rightarrow \ldots \rightarrow M_{agglomerate} \quad (4)$$

The phenomenon of electrochemical discharge in aqueous solutions is now extensively investigated as a method for obtaining of silver nanoparticles (AgNPs). Using of such a technique enables the production of AgNPs with different sizes and spectral characteristics (see Table 1). The shape of obtained AgNPs is mainly spherical, but the formation of nanosized silver dendrites is possible too [32].

Among the metals used for "cathode plasma" tungsten has the highest melting point (3422 °C). This allows the synthesis of silver nanoparticles by "cathode plasma" without destruction of the cathode. In addition, tungsten electrodes are widely used for tungsten inert gas welding. Therefore, they can be effective cathodes in the future commercialization of the proposed synthesis of silver nanoparticles.

Microplasma synthesis of AgNPs is carried out mainly in the air [18, 24, 25, 27–32] and sometimes in the inert gas atmosphere [19–21, 26, 30]. Working solutions contain surfactants based on monomeric or polymeric organic substances (stabilizers) and the soluble salts of silver are used as a source of Ag^+ (see Table 1). However, the use of silver salts makes difficult the control of nanoparticles formation process from size and shape prediction viewpoints because of the instability of metallic ions concentration in the working solution. This problem can be solved by the synthesis of AgNPs in electrolyzers equipped by soluble "sacrificial" anodes [10–13]. However, the behavior of silver "sacrificial" anodes during microplasma synthesis of AgNPs is studied insufficiently. That is why the main goals of presented work were the investigations of electrochemical behavior of silver anodes in the solutions of PVP as well as investigations of microplasma synthesis of AgNPs stabilized by PVP using sacrificial anodes and determination of adaptability of the process.

Materials and methods

Electrochemical synthesis of AgNPs

For the synthesis of AgNPs, two silver plates (2 × 3 cm, 99.99% purity) were used as anodes and tungsten (99.9% purity) wire (∅ = 0.1 mm with a working length of 5 mm) was used as cathode. The backs of silver anodes were insulated with teflon tape. Polyvinylpyrrolidone with MW = 2500 (ALSI, Authorized distributor of Sigma-Aldrich in Ukraine, Kyiv) was used as a stabilizer, NaOH (titrant, "Kharkovreachem," Kharkiv, Ukraine), and sodium acetate (NaAc, 99.9 % was purchased from "Sfera Sim," Lviv, Ukraine) were used to adjust the pH 8.

Synthesis of AgNPs was carried out in the thermostated reactor under continuous agitation with a frequency of 600–800 rpm using magnetic stirrer at 20 °C (the procedure is schematically presented in Supplemental Materials, Fig. S1). In the reactor filled by 100 mL of working solution, two silver anodes were placed and fixed at a distance of 5 cm from each other. Thereafter, the tungsten cathode was fixed at the center of surface of the solution and the current supply unit (U = 175–275 V) was connected and the glow discharge was formed.

Element analysis of obtained AgNPs solutions was carried out using portable X-ray fluorescence spectrometer ElvaX

Table 1 Characteristics of AgNPs synthesized via electrochemical discharge in aqueous solutions

Precursor	Stabilizer	Cathode	Anode	U, V	τ, min	Max. abs. peak (λ_{max}), nm	Particle size, nm	Ref
Na_3Cit	–	Silver	Silver	140	1.5	392–399	< 100	[24]
$AgNO_3$	Citrate	Titanium	Titanium	-	6	410	18	[25]
$AgNO_3$	PVP	Tungsten	Tungsten	1200, 2300	2–10	380–384	~ 3.5	[26]
$AgNO_3$	PVP	Tungsten	Tungsten	–	1.5	420	4,5	[27]
$AgNO_3$	PAN*	Stainless steel	Stainless steel	-	5	-	3-5	[28]
$AgNO_3$	Alginate	Tungsten	Tungsten	800	7	415–440	5-40	[29]
$AgNO_3$	Fructose	Stainless steel	Platinum	2000	15	402-420	10-40	[30]
$AgNO_3$	Gelatin	-	-	-	3–12	411-453	5-20	[31]
$AgNO_3$	-	Tungsten	Tungsten	800–1000	2–10	365-373	13–109	[32]

PAN, polyacrylonitrile

(Elvatech Ltd., Kyiv, Ukraine). Solutions of 5.0 g/L PVP and $AgNO_3$ with the concentrations of Ag^+ equal to 0.5×10^{-4}, 1.0×10^{-4}, and 2.0×10^{-4} mol/L were used as reference solutions for evaluating of AgNPs concentrations in obtained products.

Chemical synthesis of AgNPs

AgNPs were synthesized by reduction of Ag^+ by PVP at 70 °C at thermostated reactor equipped by magnetic stirrer and fluid-cooled condenser. To 97-mL of heated PVP solution (pH = 8) was added 3 mL of 0.01 mol/L solution of $AgNO_3$ ($AgNO_3$, 99%; ALSI, Authorized distributor of Sigma-Aldrich in Ukraine, Kyiv).

Electrochemical measurements

Polarization curves were recorded using standard a 50-ml three-electrode electrochemical cell and potentiostat PI-50-1 equipped by the programmer PR-8 and analog-to-digital converter. Silver rod (0.5 cm diameter) and platinum plate (0.75 cm^2) were used as working and auxiliary electrodes. As the reference electrodes Ag/AgCl (EVL-1M4 was purchased from "Systema Optymum," Lviv, Ukraine) mounted in a Luggin capillary contained 1 mol/L KNO_3 was used. The all values of potentials are given relative to the saturated silver chloride electrode. The scan rate of the potential was 20 mV/s in the range of *E* from 0 to + 1.0 V. The anodic behavior of silver was studied in PVP solutions from 0.5 to 10 g/L at pH = 8 and temperatures range from 20 to 50 °C.

Transmission electron microscopy analysis

TEM images of the samples were recorded using a JEM-I230 (JEOL, Tokyo, Japan) with an acceleration voltage of 80 kV. The samples for TEM investigations were prepared by drying of 0.05 μL of silver sol on the carbon grid at room temperature. The diameters of obtained AgNPs were determined using TEM images by comparison of the sizes of individual particles with the scales presented on images. The mean diameter of AgNPs and polydispersity index were calculated using Gaussian function.

Viscosity of PVP solutions

The measurements of viscosity of PVP solutions were done using Ostwald viscometer. Temperature was maintained with an accuracy of 0.1 °C. Any points have been repeated at least for 10 times and experimental errors for the all cases were less than 5%.

Kinetics of AgNPs formation

Kinetics of AgNPs formation was monitored using UV-Vis spectrophotometer UV–mini 1240 (Shimadzu Corp., Kyoto, Japan). UV-Vis spectra of reaction mixtures were recorded using a 1-cm cuvette at wavelength range from 300 to 1100 nm. Samples for spectroscopy were taken every 10 s (in the case of microplasma synthesis) or 5 min (in the case of chemical synthesis). The rates of processes (in terms s^{-1}) were evaluated by the slopes of linear parts of dependencies of maximum of absorbance of solutions on time.

Results and discussion

Electron-donor atoms of the oxygen and nitrogen of the pyrrolidone fragment of the polymer molecule of PVP can form bonds with Ag^+ ions by a donor-acceptor mechanism: O → Ag^+ and (or) N → Ag^+ [33]. Therefore, in PVP solutions, complexes with a bidentate ligand with such variants of Ag^+ localization in the polymer chain are formed:

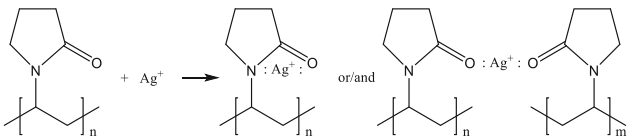

(5)

Regardless of the method of synthesis of AgNPs in PVP solutions (chemical [33, 34] or electrochemical synthesis on the surface of cathode [35]) formed Ag^0 atoms are combined into nanoclusters (AgNCs) and AgNPs according to the scheme (4). AgNPs are stabilized by donor-acceptor bonding to silver atoms O → Ag^0 and (or) N → Ag^0 forming surface complexes. Steric factor of the polymer chain of the PVP molecule also contributes to the stabilization of AgNPs [35].

Taking into account the above mentioned schemes (1–5) we can suggest that during the microplasma synthesis of AgNPs in solutions of PVP using sacrificial silver anodes the following electrochemical and physicochemical processes are carried out: ionization of silver (6); formation of $[Ag_nPVP]^{n+}$ complexes on the surface of a silver anode (7) and their transferring into bulk of solution (8); reduction of complexed Ag^+ to Ag^0 by hydrated electron (9) and subsequent formation of AgNCs and AgNPs stabilized by PVP (10).

$$Ag \rightarrow Ag^+_{ads} + e^- \quad (6)$$

$$nAg^+_{ads} + PVP_{ads} \rightarrow [Ag_nPVP]^{n+}_{ads} \quad (7)$$

$$[Ag_nPVP]^{n+}_{ads} \rightarrow [Ag_nPVP]^{n+}_{solution} \quad (8)$$

$$[Ag_nPVP]^{n+}_{solution} + ne^-_{aq} \rightarrow [Ag(0)_nPVP]_{solution} \quad (9)$$

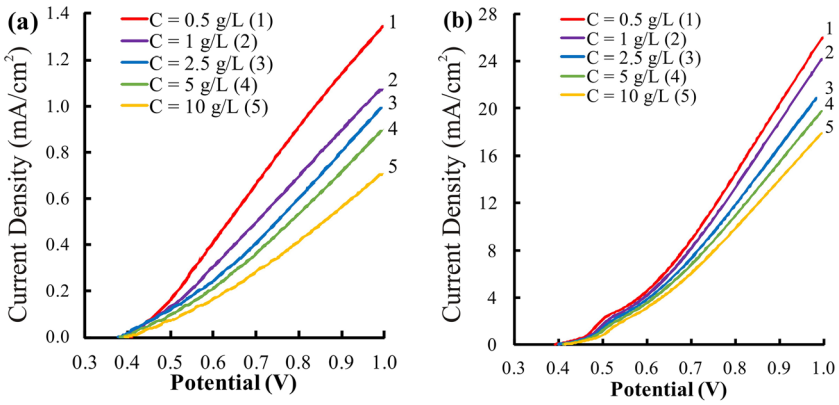

Fig. 1 Anodic polarization curves of silver in PVP–NaOH (**a**) and PVP–NaAc (**b**) solutions at different concentrations of PVP. Temperature was 20 °C

$$\left[\mathrm{Ag}(0)_n\mathrm{PVP}\right]_{\mathrm{solution}} \rightarrow \mathrm{AgNCs\ (PVP)} \rightarrow \mathrm{AgNPs\ (PVP)} \quad (10)$$

Anode dissolution of silver in PVP solutions

Anodic reactions (6–8) initiate the electrochemical synthesis of AgNPs in PVP solutions. The rates of these reactions depend on the following basic parameters: pH, surfactant concentration, voltage and temperature. Accordingly, such parameters affect the processes (9, 10) and, therefore, the total process of plasma synthesis of colloidal solutions of silver nanoparticles. Herein the effect of the concentration of PVP and temperature of the solutions on the voltammetric characteristics (namely on the values of the anode currents, i.e., on the rates of dissolution of silver in an aqueous solutions of surfactant) were investigated.

The nature of the anodic dissolution of silver in aqueous solutions of PVP–NaOH and PVP–NaAc is some different as it is indicated by the polarization curves obtained by the anodic polarization of Ag in these solutions under different conditions. Thus, the rate of anodic dissolution of metal in solutions of PVP–NaAc is much higher in comparison to the solutions of PVP–NaOH (Figs. 1, 3, and 4).

The effect of PVP concentration

The values of anode currents are decreased with increasing of concentration of PVP in solution (Fig. 1) that may be caused by the increasing of viscosity (Fig. 2a). In addition the complexes of PVP and silver ions ($[\mathrm{Ag_nPVP}]^{n+}{}_{\mathrm{ads}}$ and $[\mathrm{Ag_nPVP}]^{n+}{}_{\mathrm{solution}}$) which are formed by intermolecular interaction (5) are increased in size with increasing PVP concentration that leads to decreasing of mobility of complexes and, respectively, to slowing down of diffusion in the anode layer.

In PVP–NaAc solutions the polarization plots show an initial high dissolution followed by some degree of passivation to give the appearance of a peak at about 0.5 V that is not evident in the NaOH solutions (Fig. 1). Such a fact we can explain by following assumptions. Anode processes in addition to ionization of silver (6) include adsorption of polar PVP molecules on the anode surface and subsequent formation of $[\mathrm{Ag_nPVP}]^{n+}$ complexes (7). As we can see, the values of current in PVP–NaAc solutions are much higher than in PVP–NaOH that meant the higher concentration of $[\mathrm{Ag_nPVP}]^{n+}$ and such a complex may passivate the surface of silver at low values of potential. But such assumptions need more detailed investigations.

The effect of temperature

The rate of anodic dissolution of silver in PVP–NaOH and PVP–NaAc solutions is increased with increasing of temperature (Fig. 3). Moreover, the increasing of anode currents ($\Delta i_{\mathrm{anode}}$) for every 10° (excepting the interval from 30 to 40 °C for PVP–NaOH) is equal to about 20% that indicates the

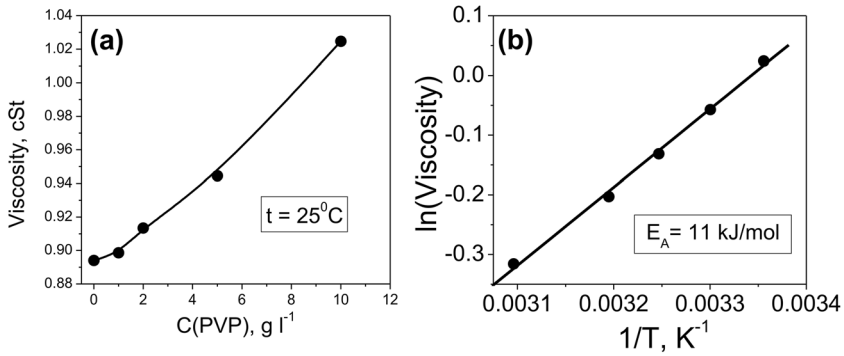

Fig. 2 Dependencies of viscosity of PVP–NaAc solution on concentration of PVP (**a**) and temperature (**b**)

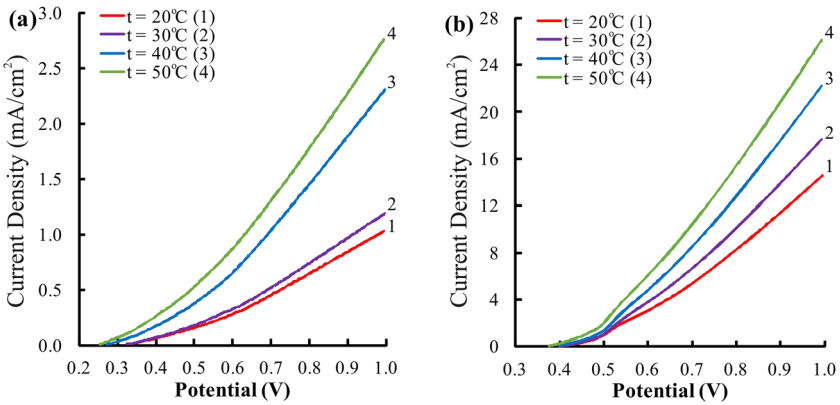

Fig. 3 Anodic polarization curves of silver in PVP–NaOH (**a**) and PVP–NaAc (**b**) solutions at different temperatures. Concentration of PVP was 5 g/L

predominant of diffusion-controlled regime of the anodic dissolution of silver. Calculated by data presented in Fig. 3 activation energies of anodic dissolution of silver are equal to 22.3 and 15.3 kJ/mol for PVP–NaOH and PVP–NaAc solutions respectively. Increasing of anode currents may be also facilitated by the reducing of the viscosity of the PVP solutions (Fig. 2b). Higher values of E_a in PVP–NaOH solutions may be caused by formation of AgOH (Ag_2O) and passivation of anode that factor was mentioned above.

Chronoamperometry

The values of the anode currents are relatively stable in time (Fig. 4), suggesting the stability of the processes (6–8) during electrolysis in PVP–NaOH and PVP–NaAc solutions.

Therefore, the anodic dissolution of silver in the range of surfactant concentrations from 0.5 to 10 g/L at 20 °C and E = 1 V occurs at anode current densities from 0.7 to 1.4 mA/cm^2 and from 18 to 26 mA/cm^2 (or from 0.07 to 0.14 A/dm^2 and from 1.8 to 2.6 A/dm^2) in PVP–NaOH and PVP–NaAc solutions respectively (see. This is equal to the dissolution of from 0.3 to 0.6 g and from 7 to 10 g of silver per 1 A·h of electric current for anode with area of 1 dm^2. Given the large current densities of active anodic dissolution in the PVP–NaAc system, it can be considered as technological for electrochemical synthesis of complexes $[Ag_nPVP]^{n+}$ that are the precursors of synthesis of PVP stabilized silver nanoparticles.

Plasma synthesis of AgNPs in PVP solutions

The intensity of glow discharge (Fig. 5) as well as values of current (Fig. 6) are relatively stable over time. At the same time $i_{anode} \approx 7$ mA/cm^2, that does not exceed this value for active anode dissolution of silver without passivation (Fig. 4). That is why passivation of the anodes is not observed during the microplasma synthesis.

The color of the solution intensively changes in a radius of 5–10 mm from the "inflamed" tungsten cathode in the form of a "whirlwind". This indicates a short distance of solvated electrons penetration from contact glow discharge into the bulk of the solution.

Kinetics of AgNPs formation in PVP solutions

Kinetics of AgNPs formation was monitored using UV-Vis spectroscopy. It was found that obtained solutions of AgNPs are characterized by intense absorbance peak at 417 nm that is typical for PVP-stabilized silver nanoparticles [35, 36]. At the same time, it must be noted that the maximum of absorbance does not change during the synthesis (Fig. 7).

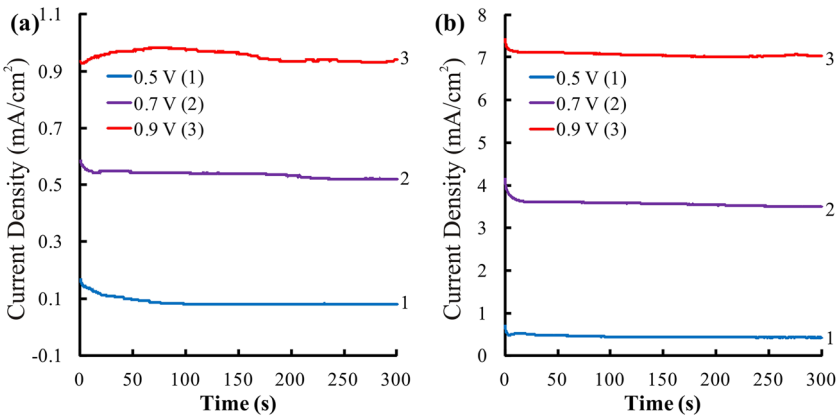

Fig. 4 Dependencies of the anode currents on time in PVP–NaOH (**a**) and PVP–NaAc (**b**) solutions at different potentials. Concentration of PVP was 5 g/L and temperature was 20 °C

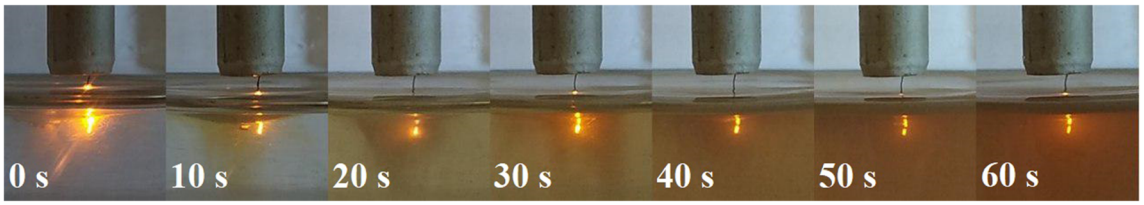

Fig. 5 Imagination of a glow discharge in solution of PVP–NaAc in time. Concentration of PVP was 5.0 g/L, pH = 8, voltage was 250 V

Using the values of optical density of solution at 417 nm (O.D.(417 nm)), the observable rate of AgNPs formation have been calculated (see insertion on Fig. 7).

It is known that PVP can reduce silver ions through the degradation of polymeric chains and formation of vinyl groups that leads to the formation of metallic silver [37]. That is why the kinetics of reduction of Ag^+ by PVP has been studied. It was found that at ambient temperature (~ 20 to 25 °C), the reaction mixture does not change color for 8 h. For that reason, the kinetics of chemical reduction of Ag^+ by PVP was investigated at 70 °C (Fig. 8).

As it was expected, the chemical reduction of Ag^+ ions by PVP even at 70 °C is very slow—the rates of processes are equal to 8.6×10^{-3} s^{-1} and 1.9×10^{-4} s^{-1} for electrochemical (at 20 °C, Fig. 7) and chemical (at 70 °C, Fig. 8) reduction of silver respectively. This finding agrees well with the above mentioned assumption on the main role of solvated electrons in the reduction of silver ions.

At the same time, it should be noted that in contrast to the electrochemical synthesis of AgNPs, some red shift of the maximum of absorbance during the chemical reduction of silver ions is observed (from 394 nm at 1500 s to 417 nm at 12000 s). Such a difference may be explained by that electrochemical reduction of Ag^+ occurs in a pseudo-stationary regime, i.e., silver ions both are reduced via reaction (10) and are formed via reaction (7). That is leads to the stability of the rates of nucleation and growth of AgNPs in time and forming of monodisperse nanoparticles (vide infra).

In the case of chemical reduction, the all nuclei of AgNPs which can be considered as $[Ag_nPVP]^{n+}$ complexes (see reactions 8 and 9) are formed directly at the reagent mixing and subsequent by nuclei growth that is reflected by the changing of the spectral characteristics—it is known [38, 39] that the position of maximum of absorbance of AgNPs solutions increase with the increasing of the size of particles.

The Uv-Vis spectra of AgNPs solutions prepared via microplasma technique can be used for evaluating of concentration of silver in obtained compositions. It is known [40] that the optical density of AgNPs solution is proportional to the silver content. The molar attenuation coefficient of chemically obtained AgNPs is equal to 6000 L/(mol·cm) (or 56 L/(g·cm)) and such value is in good agreement with presented in [38]. Taking into account the same positions of maximum of absorbance of AgNPs solutions obtained by chemical and electrochemical techniques, we can calculate the concentration of Ag in the solution after 1 min of microplasma treatment which is equal to 10 mg/L. Calculated via UV-Vis spectra value of AgNPs concentration is in good agreement with the results of element analysis of obtained solution (12 mg/L). At the same time, it should be noted that concentration of microplasma synthesized AgNPs in solutions does not depend on concentration of PVP which confirms the main role of hydrated electrons in the reaction of Ag^+ reduction.

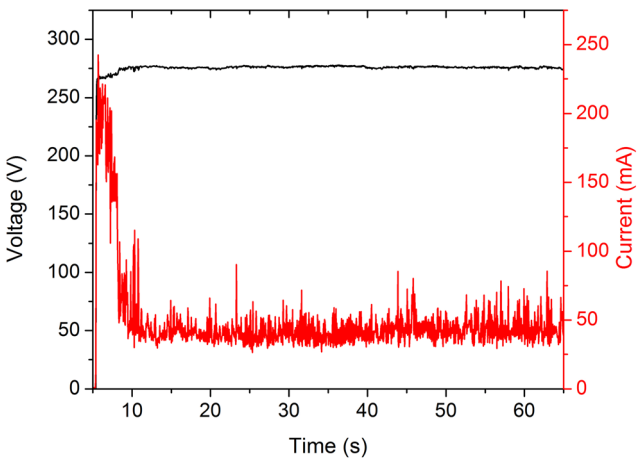

Fig. 6 Changing of values of current and voltage over time during glow discharge in PVP–NaAc solution. Conditions are the same as presented on Fig. 5

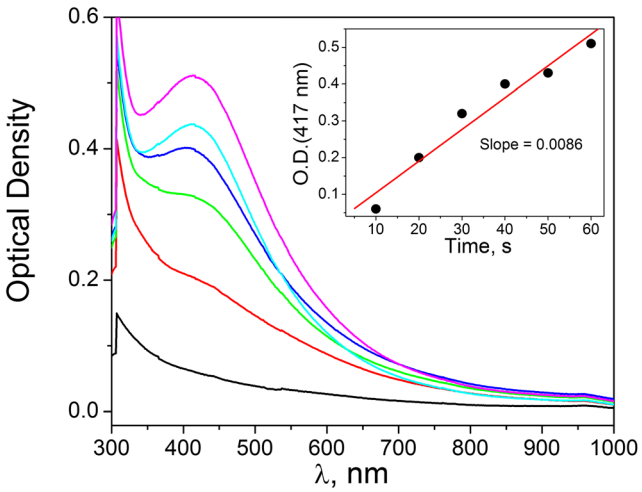

Fig. 7 The Uv-Vis spectra of AgNPs solutions at the different times of electrolysis. Insertion is the dependency of optical densities at 417 nm on time. Synthesis conditions are the same as noted in Fig. 5

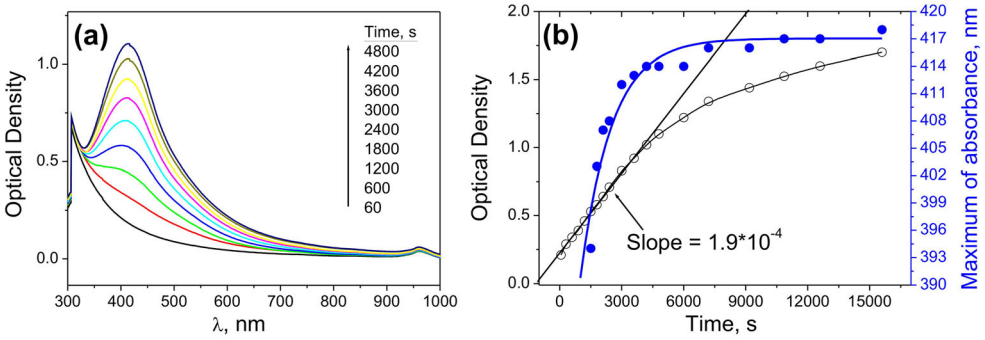

Fig. 8 The Uv-Vis spectra of AgNPs solutions at the different times of chemical reduction of $AgNO_3$ by PVP (**a**) and the dependencies of optical density at the maximum of absorbance (hollow circles) and the positions of maximum of absorbance of solutions (blue circles) on time (**b**)

Additionally, as we can see from Fig. 7, the rate of AgNPs formation by microplasma technique is equal to 0.16 mg/(L·s). Such value is a few orders of magnitude higher than the rate of AgNPs formation via Ag^+ reduction by hydroquinone [41] or hydrazine hydrate [42]. Taking into account, a very high rate of AgNPs' formation that excludes any degradations of stabilizer as well as the absence of tungsten contaminations (see "Electrochemical synthesis of AgNPs"), we can assume that obtained solutions consist of only the stabilizer, pH-regulating agent and AgNPs.

TEM investigations of electrochemically synthesized AgNPs

AgNPs obtained by contact glow discharge in 2.5, 5, and 10 g/L PVP solutions have been investigated using TEM, and it was found that the mean size of particles decrease with increasing of PVP concentration from ~ 11 to ~ 5 nm. Such fact was expected and it is in good agreement with the references [37, 41].

At the same time, one important point must be noted. As we can see from Fig. 9, the changing of size distributions of particles are non-monotonous. That is, for the concentration of PVP equal to 5 g/L, the mean diameter of particles is equal to 9 nm and particles are characterized by narrow size distribution (8.9 ± 1.3 nm, the fraction of particles from 8 to 10 nm is more than 75%). So, obtained AgNPs may be considered as monodisperse. For the concentration of PVP equal to 2.5 g/L, the mean diameter of particles is equal to 10 nm and the size distribution is wider (10.1 ± 3.6 nm), but the fraction of particles from 9 to 12 nm is still higher than 75%. And for the high (10 g/L) concentration of PVP, we can observe bimodal size distribution function that characterized by maximums at 5 nm (5.1 ± 1.2 nm) and 11 nm (11 ± 6 nm). The appropriate

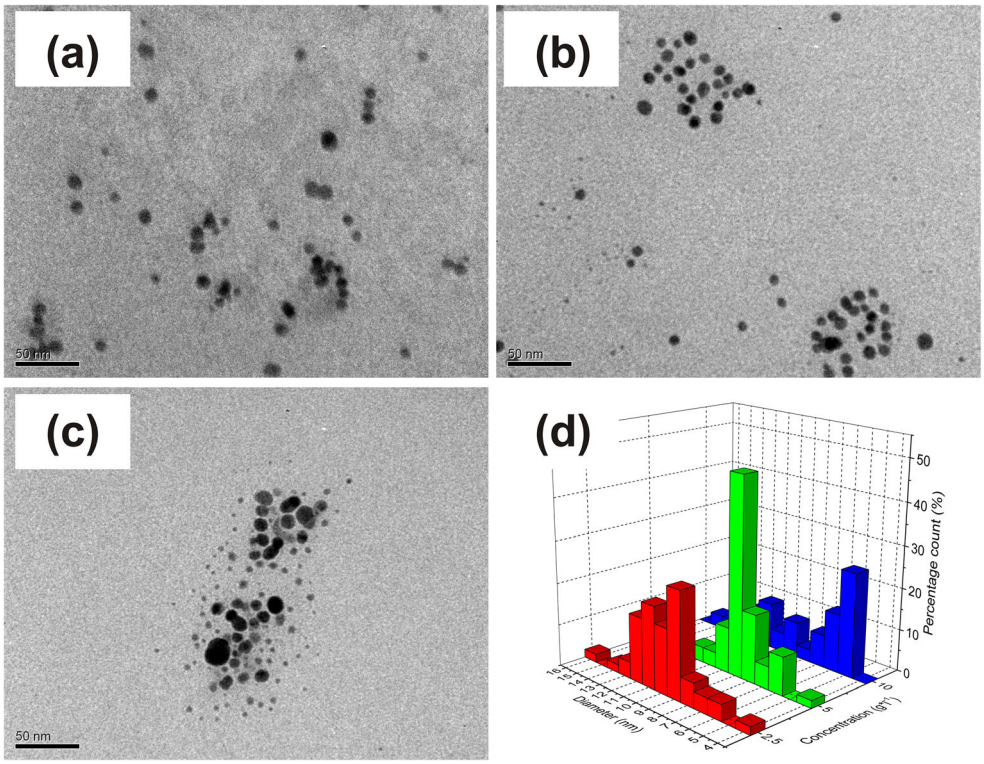

Fig. 9 TEM-images of AgNPs obtained by contact glow discharge during 2 min in solutions of PVP (g/L): 2.5 (**a**), 5.0 (**b**), 10.0 (**c**), and the size distribution histograms (**d**)

2D histograms with Gaussian optimizations are presented in Supplementary Materials (Fig. S2).

Such a nonmonotonicity of changing of AgNPs characteristics may be explained in the terms of reactions (6)–(10). At the first, as it is shown on Fig. 1b, the values of current density for 2.5, 5, and 10 g/L of PVP are close then the concentrations of Ag^+ in these solutions will be close too. That is, why the rate of nucleation will be determined by the concentration of PVP (see eqs. 8 and 9 subsequent by 10). Increasing of rate of nucleation leads to increasing of number of nuclei and, respectively, to increasing of number of formed AgNPs and decreasing of their mean size. This decrease of the average size of AgNPs we observe in the histograms (Fig. 9d)—decreasing of mean size from 11 to 5 nm (first maximum) for 2.5 and 10 g/L of PVP respectively. At the same time, the second maximum on the histogram (~ 11 nm) for concentration of PVP equal to 10 g/L may be caused by increasing of concentration of small silver clusters as well as possible interaction of polymeric balls in concentrated PVP solution that leads to increase the probability of the aggregation and formation of AgNPs with irregular shape (see Fig. 9c).

Conclusions

We fabricated PVP-stabilized silver nanoparticles using express technique of reduction of Ag^+ by solvated electrons generated by microplasma and using "sacrificial" anodes as a source of silver ions. Using voltammetry investigations of Ag anodic dissolution, (1) it was shown the stability of anodes in time that caused by complexing of Ag^+ and PVP; (2) it was found that dissolution of silver anodes is controlled by diffusion. Based on kinetic data associated with TEM investigations, the multistage mechanism of microplasma synthesis of AgNPs is proposed. Such mechanism includes the ionization of silver, the formation of [Ag^+–PVP] complexes on the surface of a silver anodes and their transferring in bulk of solution followed by reduction of complexed Ag^+ to Ag^0 by hydrated electrons and subsequent formation of AgNPs stabilized by PVP. The optimal conditions of fabrication of nearly monodisperse (the fraction of particles from 8 to 10 nm is more than 75%) AgNPs have been determined. Such optimal conditions are the background for "green" technology of continuous-flow synthesis of colloidal solutions of AgNPs.

Supplementary Information The online version contains supplementary material available at https://doi.org/10.1007/s00396-021-04811-y.

Funding This work was carried out with the partial financial support of the National Research Foundation of Ukraine (Agreement 165/02.2020).

Compliance with ethical standards

Conflict of interest The authors declare that they have no conflict of interest.

References

1. Natsuki J, Natsuki T, Hashimot Y (2015) A review of silver nanoparticles: synthesis methods, properties and applications. Int J Mater Sci Appl 4:325–332. https://doi.org/10.11648/j.ijmsa.20150405.17
2. Paramasivam G, Kayambu N, Rabel AM, Sundramoorthy AK, Sundaramurthy A (2017) Anisotropic noble metal nanoparticles: synthesis, surface functionalization and applications in biosensing, bioimaging, drug delivery and theranostics. Acta Biomater 49:45–65. https://doi.org/10.1016/j.actbio.2016.11.066
3. Zhang Z, Shen W, Xue J, Liu Y, Liu Y, Yan P, Liu J, Tang J (2018) Recent advances in synthetic methods and applications of silver nanostructures. Nanoscale Res Lett 13:54. https://doi.org/10.1186/s11671-018-2450-4
4. Chaiendoo K, Boonchiangma S, Promarak V, Ngeontae W (2018) New sensitive strategy for formaldehyde sensing by in situ generation of luminescent silver nanoclusters. Colloid Polym Sci 296(12):1995–2004. https://doi.org/10.1007/s00396-018-4427-3
5. Srikar SK, Giri DD, Pal DB, Mishra PK, Upadhyay SN (2016) Green synthesis of silver nanoparticles: a review. Green Sustain Chem 6:34–56. https://doi.org/10.4236/gsc.2016.61004
6. Pareek V, Bhargava A, Gupta R, Jain N, Panwar J (2017) Synthesis and applications of noble metal nanoparticles: a review. Adv Sci Eng Med 9:527–544. https://doi.org/10.1166/asem.2017.2027
7. Besenhard MO, Baber R, LaGrow AP, Mazzei L, Thanh NTK, Gavriilidis A (2018) New insight into the effect of mass transfer on the synthesis of silver and gold nanoparticles. CrystEngComm 20:7082–7093. https://doi.org/10.1039/c8ce01014e
8. Xi Z, Ye H, Xia X (2018) Engineered noble-metal nanostructures for in vitro diagnostics. Chem Mater 30:8391–8414. https://doi.org/10.1021/acs.chemmater.8b04152
9. Kinnear C, Moore TL, Rodriguez-Lorenzo L, Rothen-Rutishauser B, Petri-Fink A (2017) Form follows function: nanoparticle shape and its implications for nanomedicine. Chem Rev 117:11476–11521. https://doi.org/10.1021/acs.chemrev.7b00194
10. Fox CM, Yu T, Breslin CB (2020) Electrochemical formation of silver nanoparticles and their catalytic activity immobilised in a hydrogel matrix. Colloid Polym Sci 298:549–558. https://doi.org/10.1007/s00396-020-04624-5
11. Blandón L, Vázquez MV, Benjumea DM, Ciro G (2012) Electrochemical synthesis of silver nanoparticles and their potential use as antimicrobial agent: a case study on *Escherichia coli*. Port Electrochim Acta 30(2):135–144. https://doi.org/10.4152/pea.201202135
12. Dobre N, Petica A, Buda M, Anicăi L, Vişan T (2014) Electrochemical synthesis of silver nanoparticles in aqueous electrolytes. UPB Sci Bull Ser B 76:127–136
13. Yanilkin VV, Nasretdinova GR, Kokorekin VA (2018) Mediated electrochemical synthesis of metal nanoparticles. Russ Chem Rev 87:1080–1110. https://doi.org/10.1070/RCR4827
14. Kuntyi OI, Kytsya AR, Mertsalo IP, Mazur AS, Zozula GI, Bazylyak LI, Topchak RV (2019) Electrochemical synthesis of silver nanoparticles by reversible current in solutions of sodium polyacrylate. Colloid Polym Sci 297:689–695. https://doi.org/10.1007/s00396-019-04488-4
15. Kuntyi O, Mazur A, Kytsya A, Karpenko O, Bazylyak L, Mertsalo I, Pokynbroda T, Prokopalo A (2020) Electrochemical synthesis of silver nanoparticles in solutions of rhamnolipid. Micro Nano Lett 15(12):802–807. https://doi.org/10.1049/mnl.2020.0195
16. Toriyabe Y, Watanabe S, Yatsu S, Shibayama T, Mizuno T (2007) Controlled formation of metallic nanoballs during plasma electrolysis. Appl Phys Lett 91:041501–041503. https://doi.org/10.1063/1.2760042

17. Lal A, Bleuler H, Wüthrich R (2008) Fabrication of metallic nanoparticles by electrochemical discharges. Electrochem Commun 10: 488–491. https://doi.org/10.1016/j.elecom.2008.01.017
18. Wüthrich R, Allagui A (2010) Building micro and nanosystems with electrochemical discharges. Electrochim Acta 55:8189–8196. https://doi.org/10.1016/j.electacta.2010.01.096
19. Tochikubo F, Shimokawa Y, Shirai N, Uchida S (2014) Chemical reactions in liquid induced by atmospheric-pressure dc glow discharge in contact with liquid. Jpn J Appl Phys 53:126201–126208. https://doi.org/10.7567/JJAP.53.126201
20. Shirai N, Uchida S, Tochikubo F (2014) Synthesis of metal nanoparticles by dual plasma electrolysis using atmospheric dc glow discharge in contact with liquid. Jpn J Appl Phys 53:046202–046205. https://doi.org/10.7567/JJAP.53.046202
21. Oka Y, Kuroshima T, Sawachika K, Yamashita M, Sakao M, Ohnishi K, Asami K, Yatsuzuka M (2019) Preparation of silver nanocolloidal solution by cavitation bubble plasma. Vacuum 167: 530–535. https://doi.org/10.1016/j.vacuum.2018.05.013
22. Rumbach P, Go DB (2017) Perspectives on plasmas in contact with liquids for chemical processing and materials synthesis. Top Catal 60:799–811. https://doi.org/10.1007/s11244-017-0745-9
23. Lin L, Starostin SA, Li S, Hessel V (2018) Synthesis of metallic nanoparticles by microplasma. Phys Sci Rev 3:1–91. https://doi.org/10.1515/psr-2017-0121
24. Tseng K-H, Chen YC, Shyue JJ (2011) Continuous synthesis of colloidal silver nanoparticles by electrochemical discharge in aqueous solutions. J Nanopart Res 13:1865–1872. https://doi.org/10.1007/s11051-010-9937-y
25. Ashkarran AA (2010) A novel method for synthesis of colloidal silver nanoparticles by arc discharge in liquid. Curr Appl Phys 10: 1442–1447. https://doi.org/10.1016/j.cap.2010.05.010
26. Zhang YT, Guo Y, Ma TC (2011) Plasma catalytic synthesis of silver nanoparticles. Chin Phys Lett 28:105201–105203. https://doi.org/10.1088/0256-307X/28/10/105201
27. Sato S, Mori K, Ariyada O, Atsushi H, Yonezawa T (2011) Synthesis of nanoparticles of silver and platinum by microwave-induced plasma in liquid. Surf Coat Technol 206:955–958. https://doi.org/10.1016/j.surfcoat.2011.03.110
28. Shi Q, Vitchuli N, Nowak J, Caldwell JM, Breidt F, Bourham M, Zhang X, McCord M (2011) Durable antibacterial Ag/polyacrylonitrile (Ag/PAN) hybrid nanofibers prepared by atmospheric plasma treatment and electrospinning. Eur Polym J 47: 1402–1409. https://doi.org/10.1016/j.eurpolymj.2011.04.002
29. Nam S, Ali DM, Kim J (2016) Characterization of alginate/silver nanobiocomposites synthesized by solution plasma process and their antimicrobial properties. J Nanomater 2016:1–9. https://doi.org/10.1155/2016/4712813
30. Huang XZ, Zhong XX, Lu Y, Li YS, Rider AE, Furman SA, Ostrikov K (2013) Plasmonic Ag nanoparticles via environment-benign atmospheric microplasma electrochemistry. Nanotechnol 24:095604. https://doi.org/10.1088/0957-4484/24/9/095604
31. Kim SC, Kim SM, Yoon GJ, Nam SW, Lee SY, Kim JW (2014) Gelatin-based sponge with Ag nanoparticles prepared by solution plasma: fabrication, characteristics, and their bactericidal effect. Curr Appl Phys 14:S172–S179. https://doi.org/10.1016/j.cap.2013.12.032
32. Jin SH, Kim SM, Lee SY, Kim JW (2014) Synthesis and characterization of silver nanoparticles using a solution plasma process. J Nanosci Nanotechnol 14:8094–8097. https://doi.org/10.1166/jnn.2014.9428
33. Zhang Z, Zhao B, Hu L (1996) PVP protective mechanism of ultrafine silver powder synthesized by chemical reduction processes. J Solid State Chem 121:105–110. https://doi.org/10.1006/jssc.1996.0015
34. Malina D, Sobczak-Kupiec A, Wzorek Z, Kowalski Z (2012) Silver nanoparticles synthesis with different concentrations of polyvinylpyrrolidone. Dig J Nanomater Biostruct 7:1527–1534
35. Yin B, Ma H, Wang S, Chen S (2003) Electrochemical synthesis of silver nanoparticles under protection of poly(N-vinylpyrrolidone). J Phys Chem B 107:8898–8904. https://doi.org/10.1021/jp0349031
36. Wang H, Qiao X, Chen J, Wang X, Ding S (2005) Mechanisms of PVP in the preparation of silver nanoparticles. Mater Chem Phys 94(2-3):449–453. https://doi.org/10.1016/j.matchemphys.2005.05.005
37. Hoppe CE, Lazzari M, Pardinas-Blanco I, López-Quintela MA (2006) One-step synthesis of gold and silver hydrosols using poly (N-vinyl-2-pyrrolidone) as a reducing agent. Langmuir 22:7027–7034. https://doi.org/10.1021/la060885d
38. Slistan-Grijalva A, Herrera-Urbina R, Rivas-Silva JF, Ávalos-Borja M, Castillón-Barraza FF, Posada-Amarillas A (2005) Classical theoretical characterization of the surface plasmon absorption band for silver spherical nanoparticles suspended in water and ethylene glycol. Phys E 27:104–112. https://doi.org/10.1016/j.physe.2004.10.014
39. Kytsya AR, Reshetnyak OV, Bazylyak LI, Hrynda YM (2014) UV/VIS-spectra of silver nanoparticles as characteristics of their sizes and sizes distribution. In: Zaikov GE, Bazylyak LI, Haghi AK (eds) Functional polymer blends and nanocomposites: a practical engineering approach1st edn. Apple Academic Press, New York, pp 231–239. https://doi.org/10.1201/b16895
40. Sandoe HE, Watzky MA, Diaz SA (2019) Experimental probes of silver metal nanoparticle formation kinetics: comparing indirect versus more direct methods. Int J Chem Kinet 51:861–871. https://doi.org/10.1002/kin.21315
41. Patakfalvi R, Papp S, Dekany I (2007) The kinetics of homogeneous nucleation of silver nanoparticles stabilized by polymers. J Nanopart Res 9:353–364. https://doi.org/10.1007/s11051-006-9139-9
42. Kytsya A, Bazylyak L, Simon P, Zelenina I, Antonyshyn I (2019) Kinetics of Ag300 nanoclusters formation: the catalytically effective nucleus via a steady-state approach. Int J Chem Kinet 51:266–273. https://doi.org/10.1002/kin.20913